HHS Public Access

Author manuscript

Biomed Pharmacother. Author manuscript; available in PMC 2017 August 11.

Published in final edited form as:

Biomed Pharmacother. 2017 May ; 89: 146–151. doi:10.1016/j.biopha.2017.02.003.

Technetium-99 m radiolabeled paclitaxel as an imaging probe for breast cancer *in vivo*

Liziane O.F. Monteiro[a], **Renata S. Fernandes**[a], **Luciano C. Castro**[a], **Valbert N. Cardoso**[b], **Mônica C. Oliveira**[a], **Danyelle M. Townsend**[c], **Alice Ferretti**[d], **Domenico Rubello**[d,*], **Elaine A. Leite**[a], and **André L.B. de Barros**[b,*]

[a]Department of Pharmaceutical Products, Faculty of Pharmacy, Universidade Federal de Minas Gerais, Belo Horizonte, Minas Gerais, Brazil

[b]Department of Clinical and Toxicological Analyses, Faculty of Pharmacy, Universidade Federal de Minas Gerais, Belo Horizonte, Minas Gerais, Brazil

[c]Department of Drug Discovery and Pharmaceutical Sciences, Medical University of South Carolina, USA

[d]Department of Nuclear Medicine, Molecular Imaging, Radiology, Neuro Radiology, Medical Physics, Clinical Laboratory, Microbiology & Pathology, Santa Maria de la Misericordia Hospital, Rovigo, Italy

Abstract

The high incidence and mortality of breast cancer supports efforts to develop innovative imaging probes to effectively diagnose, evaluate the extent of the tumor, and predict the efficacy of tumor treatments while concurrently and selectively delivering anticancer agents to the cancer tissue. In the present study we described the preparation of technetium–99 m (^{99m}Tc)-labeled paclitaxel (PTX) and evaluated its feasibility as a radiotracer for breast tumors (4T1) in BALB/c mice. Thin Layer Chromatography (TLC) was used to determine the radiochemical purity and *in vitro* stability of ^{99m}Tc-PTX. PTX micelles showed a unimodal distribution with mean diameter of 13.46 ± 0.06 nm. High radiochemical purity (95.8 ± 0.3%) and *in vitro* stability (over than 95%), up to 24 h, were observed. Blood circulation time of ^{99m}Tc-PTX was determined in healthy BALB/c mice. ^{99m}Tc-PTX decays in a one-phase manner with a half-life of 464.3 minutes. Scintigraphic images and biodistribution were evaluated at 4, 8 and 24 h after administration of ^{99m}Tc-PTX in 4T1 tumor-bearing mice. The data showed a significant uptake in the liver, spleen and kidneys, due to the importance of these routes for excretion. Moreover, high tumor uptake was achieved, indicated by high tumor-to-muscle ratios. These findings indicate the usefulness of ^{99m}Tc-PTX as a radiotracer to identify 4T1 tumor in animal models. In addition, ^{99m}Tc-PTX might be used to follow-up treatment protocols in research, being able to provide information about tumor progression after therapy.

*Corresponding authors. Domenico.rubello@libero.it (D. Rubello), brancodebarros@yahoo.com.br (A.L.B. de Barros).

Conflicts of interest

Authors declare that they have no conflicts of interest.

Keywords

Breast cancer; Scintigraphic images; Biodistribution profile; 4T1 tumor; Paclitaxel

1. Introduction

Nuclear medicine is characterized by a non-invasive imaging approach for visual assessment and quantitative measurement of molecular and biochemical properties of cells, including tumor cells. Several radionuclides are used in nuclear medicine, including iodine-131, indium-111, thallium-201, fluorine-18, technetium-99m, galium-67, among others [4,5]. One of the most common radiotracers for imaging is the technetium–99 m (^{99m}Tc). This isotope has suitable physical and chemical characteristics, including a physical half-life of 6.02 h and gamma emission of low energy (140 keV) with the added advantage of abundant availability in nuclear medicine laboratories and low cost [6–9].

Due to the high incidence and mortality of breast cancer, efforts should be done in order to develop new probes to effectively diagnose, evaluate the extent of the tumor, and predict the efficacy of tumor treatments in clinical and pre-clinical trials. In this context, a large number of candidate probes labeled with ^{99m}Tc have been reported, including peptides, nanoparticles, carbohydrates, and anticancer drugs [5,10–13].

Paclitaxel (PTX) is one of the most effective and most-widely used antitumor drugs with clinical efficacy against a wide range of solid tumors, including ovarian, non-small cell lung cancer, and head and neck tumors. PTX is a first-line treatment for patients with metastatic breast cancer. However, PTX is poorly soluble in water, which represents a barrier for intravenous administration [14–16]. The commercially available preparation of PTX, Taxol®, is a micellar dispersion, composed by a 1:1 blend of Cremophor EL® (polyethoxylated castor oil) and dehydrated ethanol, which is diluted (5–20 times) in saline or dextrose solution (5%) for *in vivo* administration [17,18]. In a micellar dispersion, tumor accumulation is favored by the enhanced permeation and retention (EPR) effect, due to the formation of nanoscaled particles. Nanoparticles in a range of 10 to 500 nm might extravasate and accumulate into tumors due to the presence of large gaps between endothelial cells allied to the impaired lymphatic drainage [19–22]. Furthermore, PTX dispersion has functional groups that are able to form complexes with ^{99m}Tc, such as —OH. In this way, PTX micellar dispersion, if radiolabeled, might be a promising radiotracer for identifying tumor, and evaluating tumor progression after treatment regimens.

Thus, in the present study, PTX micellar dispersion was radiolabeled with ^{99m}Tc and *in vitro* radiochemical stability was determined. In addition, blood circulation time was evaluated in healthy mice. Biodistribution studies and scintigraphic images were performed to demonstrate the feasibility of ^{99m}Tc-PTX as a radiotracer for breast tumor (4T1) in BALB/c mice.

2. Material and methods

2.1. Materials

Paclitaxel was supplied by Quiral Quimica do Brasil S.A (Juiz de Fora, Brazil). Cremophor EL®, $SnCl_2$•$2H_2O$ and trypsin-EDTA solution (0.5%) were purchased from Sigma-Aldrich (São Paulo, Brazil). ^{99m}Tc was obtained from an alumina-based ^{99}Mo/^{99m}Tc generator. All other chemicals and reagents were of analytical grade.

2.2. Cell culture 4T1

The murine 4T1 cell line was purchased from American Type Culture Collection (ATCC) (Manassas, EUA). Dulbecco's modified Eagle's medium (DMEM) were supplied by Gibco Life Technologies (Carlsbad, USA). 4T1 cells were maintained in DMEM supplemented with 10% (v/v) fetal bovine serum, penicillin (100 IU/ml), and streptomycin (100 μg/ml). Cells were kept at 37 °C in humidified air containing 5% CO_2. The cells were grown to confluence and later harvested by trypsinization. After centrifugation (5 min at 330*g*), the cells were resuspended in 1.0 ml DMEM and viability was determined with trypan blue (1:1) (Sigma-Aldrich, São Paulo, Brazil) and counted in a Newbauer chamber.

2.3. Paclitaxel micellar dispersion: preparation and physicochemical characterization

For micellar dispersion, 30.0 mg of PTX were solubilized in 2.0 ml of a 1:1 (v/v) dehydrated ethanol:Cremophor EL® mixture. The suspension was stirred vigorously for 5 min. Dynamic Light Scattering (DLS) with a fixed angle of 90°, using Zetasizer NanoZS90 (Malvern Instruments, England) was used to determine the mean diameter of the PTX-micelles. Samples were analyzed after 10-fold dilution in filtered 0.9% w/v NaCl solution (cellulose ester membrane, 0.45 μm, Millipore, Billerica, USA). Data were expressed as mean ± standard deviation of at least three different batches of each system.

2.4. Radiolabeling procedure and radiochemical purity evaluation

A 0.1 ml aliquot of the PTX dispersion was added to 300 μg of $SnCl_2$•$2H_2O$ in an acid solution (HCl 0.25 M) and adjusted to pH 7.4 using NaOH solution (0.1 M). A 0.1 ml aliquot of $Na^{99m}TcO_4$ (37 MBq) was added and the solution was kept at room temperature for 15 min.

Radiochemical purity was determined by Thin Layer Chromatography on silica gel (TLC-SG; Merck, Darmstadt, Germany) using acetone as mobile phase to quantify free $^{99m}TcO_4^-$. The radioactivity was determined using a Wallace Wizard 1470–020 Gamma Counter (PerkinElmer Inc., Waltham, Massachusetts, USA). The solution was purified from $^{99m}TcO_2$ using a 0.22 μm syringe filter, as previously described by Fernandes et al. [12].

2.5. *In vitro* stability: Saline and plasma

TLC-SG was used to estimate the stability of ^{99m}Tc-PTX in the presence of NaCl 0.9% (w/v), at room temperature, or murine plasma, at 37 °C. For plasma stability assessment, 90 μl of the ^{99m}Tc-PTX solution was incubated with 1.0 ml of fresh mouse plasma, under agitation, at 37 °C. Radiochemical stabilities were determined on samples taken at 1, 2, 4, 6, 8, and 24 h after incubation.

2.6. Blood clearance

Female BALB/c mice (6–8-week-old) were obtained from CEBIO-UFMG (Belo Horizonte, Brazil). All animal studies were approved by the local Ethics Committee for Animal Experiments (CEUA/UFMG) under the protocol number 268/2016. An 100 μl aliquot of ^{99m}Tc-PTX was administrated, through the tail vein, in healthy female BALB/c mice (n = 7). A small incision was made in the distal tail and blood samples (~20 μl) were collected at 5, 10, 15, 30, 45, 60, 90, 120, 240, 360, 480 and 1440 min after administration. Each sample was weighted, and the radioactivity was measured with an automatic scintillation counter. The percentage of injected dose per gram (%ID/g) in each sample was determined.

2.7. Tumor cell inoculation

An aliquot (100 μl), containing 2.5×10^6 4T1 viable cells, was injected subcutaneously into the right thigh of female BALB/c mice (17–23 g). Tumor cells were allowed to grow *in vivo* for 10 days. 4T1 tumor-bearing BALB/c mice were used for biodistribution studies and scintigraphic images.

2.8. Biodistribution studies

An aliquot (100 μl) of 3.7 MBq of ^{99m}Tc-PTX was injected intravenously into tumor-bearing BALB/c mice (n = 7). At 4, 8, and 24 h after injection, mice were anesthetized with a mixture of xylazine (10 mg/kg) and ketamine (80 mg/kg). Liver, spleen, kidneys, stomach, heart, lungs, blood, muscle, thyroid, intestine, and tumor were removed, and placed in pre-weighted plastic tubes. The radioactivity was measured using an automatic scintillation gamma counter. A standard dose containing the same injected amount was counted simultaneously in a separate tube, which was defined as 100% radioactivity. The results were expressed as the percentage of injected dose per gram of tissue (%ID/g).

2.9. Scintigraphic images

An aliquot (100 μl) of 18 MBq of ^{99m}Tc-PTX was injected intravenously into tumor-bearing BALB/c mice (n = 7). Anesthetized mice were horizontally placed under the collimator of a gamma camera (Mediso, Budapest, Hungary) coupled with a low-energy high-resolution collimator. Images were acquired at 4, 8, and 24 h after injection using a 256 × 256 × 16 matrix size, with a 20% energy window set at 140 keV for a period of 300 s each. The tumor-to-muscle ratio from the scintigraphic images were calculated for all the evaluated times.

2.10. Statistical analysis

Data were expressed as mean ± standard deviation (SD). D'agostino and Pearson and Bartlett's tests were performed to assess the normality and homogeneity of variance analysis. Data were evaluated using Student's *t*-test and one-way analysis of variance (ANOVA), followed by Tukey's test. A P-value less than 0.05 were considered to indicate a significant difference. Data were analyzed using the statistical software GraphPad PRISM, version 5.00 software (GraphPad Software Inc.).

3. Results

3.1. Particle size

The PTX micelles showed a unimodal distribution with mean diameter of 13.46 ± 0.06 nm and polydispersity index of 0.083 ± 0.005. These results indicate that micelles are suitable for intravenous administration.

3.2. Radiochemical purity and *in vitro* stability

Radiolabeling yields for ^{99m}Tc-PTX were 95.8 ± 0.3% (n > 7). TLC using acetone as mobile phase was used to quantify $^{99m}TcO_{4-}$. $^{99m}TcO_2$ was removed through sterile filters (pore diameter = 0.22 μm). In this process radiocolloids remains in the filter while $^{99m}TcO_4^-$ and ^{99m}Tc-PTX are freely filtered [12].

In vitro stabilities of ^{99m}Tc-PTX in the presence of saline, at room temperature, or plasma, at 37 °C, are depicted in Fig. 1. High stability was found (over to 95%) up to 24 h of incubation in both media. These findings, along with the high radiolabeling efficiency, suggest that ^{99m}Tc-PTX might be used for further *in vivo* assays.

3.3. Blood clearance

Blood clearance for ^{99m}Tc-PTX is shown in Fig. 2. ^{99m}Tc-PTX, after administrated into healthy female BALB/c mice, decays in a one-phase manner showing a relatively long blood circulation time of 464.3 minutes and an area under the curve of 3456.3%ID•min^{-1}.

3.4. Scintigraphic images and biodistribution studies

Scintigraphic images, acquired at 4, 8 and 24 h after ^{99m}Tc-PTX i. v. treatment in 4T1 tumor-bearing mice, are shown in Fig. 3. The complex showed significant uptake in liver and spleen due to the nanoparticles recognition by macrophages present in these organs [5,25]. Renal excretion of ^{99m}Tc-PTX was also observed. Tumor tissue could be clearly visualized on the images. The quantitative analysis of scintigraphic images is shown in Fig. 4. An increase over time was observed, reaching a maximum of 6.83 ± 0.52 at 24 h, which indicates the preferential accumulation in tumor area of ^{99m}Tc-PTX.

The biodistribution profile of ^{99m}Tc-PTX is shown in Fig. 5. As reported in the scintigraphic images, biodistribution studies showed high uptake in liver, spleen. In addition, significant uptake in kidneys and intestines, mainly at 4 h post-injection was observed. No significant accumulation was found in lungs, heart, stomach, and thyroid. It is important to note the higher tumor uptake, compared to the contralateral muscle, taken as a control was observed (Fig. 5-inset).

4. Discussion

Nuclear medicine imaging modalities, using specific targeting moieties, play a crucial role in the diagnosis, staging, and follow-up for patients with cancer. Radiotracer-based imaging approaches, such as single-photon emission computed tomography (SPECT) might provide a non-invasive *in vivo* assessment providing information about tumor localization and

progression [23,26]. The use of radionuclides combined with molecules or existing pharmaceutical compounds, such as antitumor drugs, which preferentially accumulate in tumor tissue, has significant importance since they might enable an early and more accurate diagnosis [1–3].

Among chemotherapeutic agents, PTX is one of the most effective and potent antitumor used in oncology treatment, and serves as at the forefront in metastatic breast cancer [15–22]. PTX is commercially available as a micellar dispersion in ethanol and Cremophor EL® (Taxol®) that has already been label with ^{99m}Tc for animal studies [11]. However, studies were conducted in Ehrlich Ascites tumor-bearing mice aiming to compare the tumor uptake of a new formulation. No mention was made to ^{99m}Tc-PTX, itself, as a tumor-imaging probe. Herein, we describe the procedures to radiolabel efficiently PTX with ^{99m}Tc. Stability assays were carried out in order to allow *in vivo* experiments (blood clearance, biodistribution and scintigraphic images). In addition, tumor uptake was evaluated in a 4T1 tumor model, which is widely used in pre-clinical research for testing new imaging probes and to evaluate the pharmacokinetics and antitumor activity of new potential chemotherapeutics [12,13,27]. This mammary carcinoma cell line, derivate from a spontaneously tumor in BALB/cfC3H mice, was originally isolated by Fred Miller and coworkers at the Karmanos Cancer Institute [28,29]. 4T1 cell is a highly tumorigenic cell line characterized by extensive necrosis and inflammation within the primary tumor. Furthermore, it is well described the capacity of this tumor cell line to metastasize efficiently to lungs, liver, brain and bones similarly observed in human breast cancer. Therefore, the purpose of our study was to evaluate the feasibility of ^{99m}Tc-PTX as a radiotracer to be applied as a complementary approach to monitor treatment regimens in pre-clinical studies using 4T1 tumor models. By leveraging this strategy, a variety of information might be acquired, including PTX accumulation, tumor development and tumor progression after therapy, which might be helpful to determined better treatment protocol or even to select new formulations [12,28–30].

The radiolabeling protocol to obtain ^{99m}Tc-PTX was successfully optimized to achieve high yields. It is well described that ^{99m}Tc-labeling reactions generate two main impurities, $^{99m}TcO_2$ and $^{99m}TcO_4^-$ [24,25]. The presence, in high concentration, of these entities leads to images in poor quality that might impair the correct data interpretation. According to the American Pharmacopoeia [31], radiopharmaceutical preparations are suitable for *in vivo* administration if their radioactive impurities do not exceed 10%. Therefore, by using the optimized protocol described in this study less than 5% of impurities were detected indicating that ^{99m}Tc-PTX can be used in further *in vivo* assays. Furthermore, the physiological pH obtained after labeling (pH = 7.4) is optimal for intravenous administration [24]. The presence of —OH groups in the polyethoxylated castor oil, a constituent of the Taxol formulation might explain the high labeling efficiency. It is well known that metals, including ^{99m}Tc, are stabilized by electron donating groups [32–34].

Radiolabeling stability is a mandatory characteristic for radiopharmaceutical platforms. In the event that metal detachment occurs, biodistribution and images will no longer be reliable may lead to wrong interpretations [35,36]. ^{99m}Tc-PTX showed high *in vitro* stability (over than 95%) throughout the experiment. Once injected in healthy mice, ^{99m}Tc-PTX exhibited

a relatively long half-life (464.3 minutes). Long circulation time is an important feature for nanostructured radiopharmaceuticals since a large number of passages through the targeted areas might favor radiotracer accumulation leading to better outcomes. For imaging purposes, a half-life ranging from 4 to 6 h is suitable to achieve a reasonable signal-to-noise ratio. Therefore, these findings encourage us to perform biodistribution and images studies for ^{99m}Tc-PTX in tumor-bearing mice [34,37–39,44].

As expected for a nanoparticle system, high uptake in liver and spleen were observed. This finding might be explained by the extensive phagocytosis typically experienced by nanoparticles after intravenous injection [40–42]. The substantial uptake in kidneys (Fig. 5) suggests an important elimination route of ^{99m}Tc-PTX occurs through the renal system [31–33]. Indeed, nanoparticles smaller than 10.0 nm are readily excreted through renal filtration, which might partially explain the uptake in kidneys [43]. Additionally, a significant uptake in the intestines was observed suggesting that fecal route also contribute to the excretion of ^{99m}Tc-PTX [44,45]. Noteworthy is the low uptake in thyroid and stomach, which confirms the high labeling stability showed by *in vitro* assays [24,25].

^{99m}Tc-PTX showed higher accumulation in tumor compared with control tissues, such as muscle, as evidenced by the high tumor-to-muscle ratio, mainly at 24 h post-administration (6.83 ± 0.52%). It is important to mention that a tumor-to-muscle ratio higher than 1.5, i.e, 50% more uptake in the target tissue, is required for further development of an imaging probe candidate. ^{99m}Tc-PTX showed time-dependent accumulation and tumor-to-muscle ratios superior than 1.5. This fact could be explained by the long blood circulation time, leading to more passages through the tumor region, favoring ^{99m}Tc-PTX extravasation and therefore, tumor accumulation [37–42].

5. Conclusion

PTX-micelles were successfully labeled with ^{99m}Tc in high yields and excellent stability. Due to its relatively long blood circulation time, ^{99m}Tc-PTX accumulated into 4T1 tumor tissues leading to high tumor-to-muscle ratios. Therefore, this study showed the feasibility of ^{99m}Tc-PTX as an imaging probe that can be used in the preclinical assessment of breast cancer models.

Acknowledgments

The authors would like to thank Fundação de Amparo à Pesquisa do Estado de Minas Gerais (FAPEMIG-Brazil), Conselho Nacional de Desenvolvimento Científico e tecnológico (CNPq-Brazil) and Coordenação de Aperfeiçoamento de Pessoal de Nível Superior (CAPES-Brazil) for their financial support and scholarship.

References

1. Greene LR, Wilkinson D. The role of general nuclear medicine in breast cancer. JMIRS. 2015; 62:54–65.
2. Siegel RL, Miller KD, Jemal A. Cancer statistics, 2015. CA Cancer J. Clin. 2015; 65:5–29. [PubMed: 25559415]
3. Vercher-Cornejero JL, Pelegrí-Martinez L, Lopez-Aznar D, Cózar-Santiago MP. Positron emission tomography in breast cancer. Diagnostics. 2015; 5:61–83. [PubMed: 26854143]
4. Saha, GB. Fundamentals of Nuclear Pharmacy. Springer; New York: 2010.

5. de Barros ALB, Andrade SF, Filho JDS, Cardoso VN, Alves RJ. Radiolabeling of low molecular weight D-galactose-basedglycodendrimer with technetium-99 m and biodistribution studies. J. Radioanal. Nucl. Chem. 2013; 298:605–609.
6. Yang DJ, Kim C, Schechter NR, Azhdrinia A, Yu D, Oh C. Imaging with ^{99m}Tc-ECDG targeted at the multifunctional glucose system: feasibility studies with rodents. Radiology. 2003; 226:465–473. [PubMed: 12563141]
7. Fani M, Maecke HR. Radiopharmaceutical development of radiolabelled peptides. EJNMMJ. 2012; 39:11–30.
8. De Barros ALB, Cardoso VN, Mota LG, Alves RJ. Synthesis and biodistribution studies of carbohydrate derivative radiolabeled with technetium-99m. Bioorg. Med. Chem. 2010; 20:315–317.
9. Kong FL, Zhang Y, Young DP, Yu DF, Yang DJ. Development of (99m)Tc-EC-tyrosine for early detection of breast cancer tumor response to the anticancer drug melphalan. Acad. Radiol. 2012; 20:41–51. [PubMed: 22963724]
10. Schmidt GP, Baur-Melnyk A, Haug A, Heinemann V. Comprehensive imaging of tumor recurrence in breast cancer patients using whole-body MRI at 1.5 and 3 T compared to FDG-PET-CT. Eur. J. Radiol. 2008; 65:47–58. [PubMed: 18082989]
11. Jain V, Swarnakar NK, Mishra PR, Verma A, Kaul A, Mishra AK. Paclitaxel loaded PEGylated gleceryl monooleate based nanoparticulate carriers in chemotherapy. Biomaterials. 2012; 33:7206–7220. [PubMed: 22809646]
12. Fernandes RS, Silva JO, Lopes SVA, Chondrogiannis S, Rubello D, Cardoso VN. Technetium-99m-labeled doxorubicin as an imaging probe for murine breast tumor (4T1 cell line) identification. Nucl. Med. Commun. 2016; 37:307–312. [PubMed: 26619397]
13. Silva JO, Fernandes RS, Lopes SCA, Cardoso VN, Leite EA, Cassali GD. pH-Sensitive, long-circulating liposomes as an alternative tool to deliver doxorubicin into tumors: a feasibility animal study. Mol. Imaging Biol. 2016:1–7.
14. Singla AK, Garg A, Aggarwal D. Paclitaxel and its formulations. Int. J. Pharm. 2002; 235:179–192. [PubMed: 11879753]
15. Koudelka S, Turanék J. Liposomal paclitaxel formulations. J. Control. Release. 2012; 163:322–334. [PubMed: 22989535]
16. Barbosa MV, Monteiro LOF, Carneiro G, Malagutti AR, Vilela JMC, Andrade MS, Oliveira MC, Carvalho-Júnior AD, Leite EA. Experimental design of a lipossomal lipid system: a potential strategy for paclitaxel-based breast câncer treatment. Colloids Surf. B Biointerfaces. 2015; 136:553–561. [PubMed: 26454545]
17. Surapanemi MS, Das SK, Das NG. Designing paclitaxel drug delivery systems aimed at improved patient outcomes: current status and challenges. ISRN. 2012:1–15.
18. Zhang X, Huang Y, Zhao W, Chen Y, Zhang P, Li J, Venkataramanan R, Li S. PEG- farnesyl thiosalicylic acid telodendrimer micelles as animproved formulation for targeted delivery of paclitaxel. Mol. Pharm. 2014; 11:2807–2814. [PubMed: 24987803]
19. Danhier F, Feron O, Préat V. To exploit the tumor microenvironment: passive and active tumor targeting of nanocarriers for anticancer drug delivery. J. Control. Realease. 2010; 148:135–146.
20. Maeda H, Eu J, Sawa T, Matsumura Y, Hori K. Tumor vascular permeability and the EPR effect macromolecular therapeutics: a review. J. Control. Release. 2000; 65:271–284. [PubMed: 10699287]
21. Sawant RR, Torchilin VP. Challenges in development of targeted liposomal therapeutics. AAPS. 2012; 14:303–315.
22. Ferreira DS, Lopes SCA, Franco MS, de Oliveira MC. pH-sensitive liposomes for drug delivery in cancer treatment. Ther. Deliv. 2013; 4:1–24. [PubMed: 23323774]
23. De Barros ALB, Fuscaldi LL. Radiolabeled peptides as imagins probes for cancer diagnosis. J. Mol. Pharm. Org. Process Res. 2014; 2:1–2.
24. Fuscaldi LL, dos Santos DM, Pinheiro NGS, Araújo RS, de Barros ALB, Resende JM. Synthesis and antimicrobial evaluation of two peptide LyeTx I derivatives modified with the chelating agent HYNIC for radiolabeling with technetium-99m. J. Venom. Anim. Toxins Incl. Trop. Dis. 2016; 22:1–8.

25. de Barros ALB, Mota LG, Ferreira CA, Corrêa NCR, Góes AM, Oliveira MC, et al. 99mTc-labeled bombesin analog for breast cancer identification. J. Radioanal. Nucl. Chem. 2013; 295:2083–2090.
26. Munley MT, Kagadis GC, McGee KP, Kirov AS, Jang S, Mutic S. An introduction to molecular imaging in radiation oncology: a report by the AAPM Working Group on Molecular Imaging in Radiation Oncology (WGMIR). Med. Phys. 2013; 40:1–23.
27. Fernandes RS, Silva JO, Monteiro LOF, Leite EA, Cassali GD, Rubello D. Doxorubicin-loaded nanocarriers: a comparative study of liposome and nanostructured lipid carrier as alternatives for cancer therapy. Biomed. Pharmacother. 2016; 84:252–257. [PubMed: 27664949]
28. DuPré SA, Redelman D, Hunter KW. The mouse mammary carcinoma 4T1: characterization of the cellular landscape of primary tumors and metastatic tumor foci. Int. J. Exp. Path. 2007; 88:351–360. [PubMed: 17877537]
29. Garcia CMS, Araujo MR, Lopes MTP. Morphological and immunophenotipical characterization of murine mammary carcinoma 4t1. Braz. J. Vet. Pathol. 2014; 7:158–165.
30. Tao K, Fang M, Alroy J, Sahagian GG. Imagable 4T1 model for the study of late stage breast cancer. BMC Cancer. 2008; 8:1–20. [PubMed: 18173856]
31. The United States Pharmacopoeia National Formulary. Rockville: United States Pharmacopoeial Convention Inc.; 2012. USP 34.
32. Tisato F, Refosco F, Bandoli G. Structural survey of technetium complexes. Coord. Chem. Rev. 1994; 32:5–397.
33. Gelderblom H, Verweij J, Nooter K, Sparreboom A. Cremophor EL: the drawbacks and advantages of vehicle selection for drug formulation. Eur. J. Cancer. 2001; 37:1590–1598. [PubMed: 11527683]
34. Kumar P, Singh B, Sharma S, Ghai A, Chuttani K, Mishra AK. Preclicnical evaluation of [^{99m}Tc]-labeled doxorubicin as a potential scintigraphic probe for tumor imaging. Cancer Biother. Radiopharm. 2011; 27:221–225.
35. Saha, GB. Fundamentals of Nuclear Pharmacy. Springer; New York: 2010.
36. Zhu X, Li J, Hong Y, Kimura RH, Ma X, Liu H, et al. 99mTc-labeled cysteine knot peptide targeting integrin $\alpha_v\beta_6$ for tumor SPECT imaging. Mol. Pharm. 2014; 11:1208–1217. [PubMed: 24524409]
37. Phillips WT. Delivery of gamma-imaging agents by liposomes. Adv. Drug Deliv. Rev. 1999; 37:13–32. [PubMed: 10837724]
38. Varshney R, Sethi SK, Hazari PP, Chuttani K, Soni S, Milton MD. Synthesis of [DTPA-bis(D-ser)] chelate (DBDSC): an approach for the design of SPECT radiopharmaceuticals based on technetium. Curr. Radiopharm. 2012; 5:348–355. [PubMed: 22642421]
39. Pearson RM, Vanessa VJ, Seungpyo H. Biomolecular Corona on nanoparticles: a survey of recent literature and its implications in targeted drug delivery. Front. Chem. 2014; 2:1–7.
40. Awasthi VD, Garcia D, Goins BA, Phillips V. Circulation and biodistribution profiles of long-circulating PEG-liposomes of various sizes in rabbits. Int. J. Pharm. 2003; 253:121–132. [PubMed: 12593943]
41. Soares DCF, de Oliveira MC, de Barros ALB, Cardoso VN, Ramaldes GA. Liposomes radiolabeled with ^{159}Gd: in vitro cytotoxic antitumoral activity, biodistribution study and scintigraphic image in Ehrlich tumor bearing mice. Eur. J. Pharm. Sci. 2011; 43:290–296. [PubMed: 21605669]
42. De Barros ALB, Mota LG, Coelho MMA, Corrêa NCR, Góes AM, Oliveira MC. Bombesin encapsulated in long-circulating pH-sensitive liposomes as a radiotracer for breast tumor identification. J. Biomed. Nanotechnol. 2015; 11:342–348. [PubMed: 26349310]
43. Miyata K, Christie RJ, Kataoka K. Polymeric micelles for nano-scale drug delivery. React. Funct. Polym. 2011; 71:227–234.
44. Vaishampayan U, Parchment RE, Jasti BR, Taxanes Hussain M. An overview of the pharmacokinetics and pharmacodynamics. Urology. 1999; 54:22–29. [PubMed: 10606281]
45. Barbuti AM, Chen Z. Paclitaxel through the ages of anticancer therapy: exploring its role in chemoresistance and radiation therapy. Cancers. 2015; 7:2360–2371. [PubMed: 26633515]

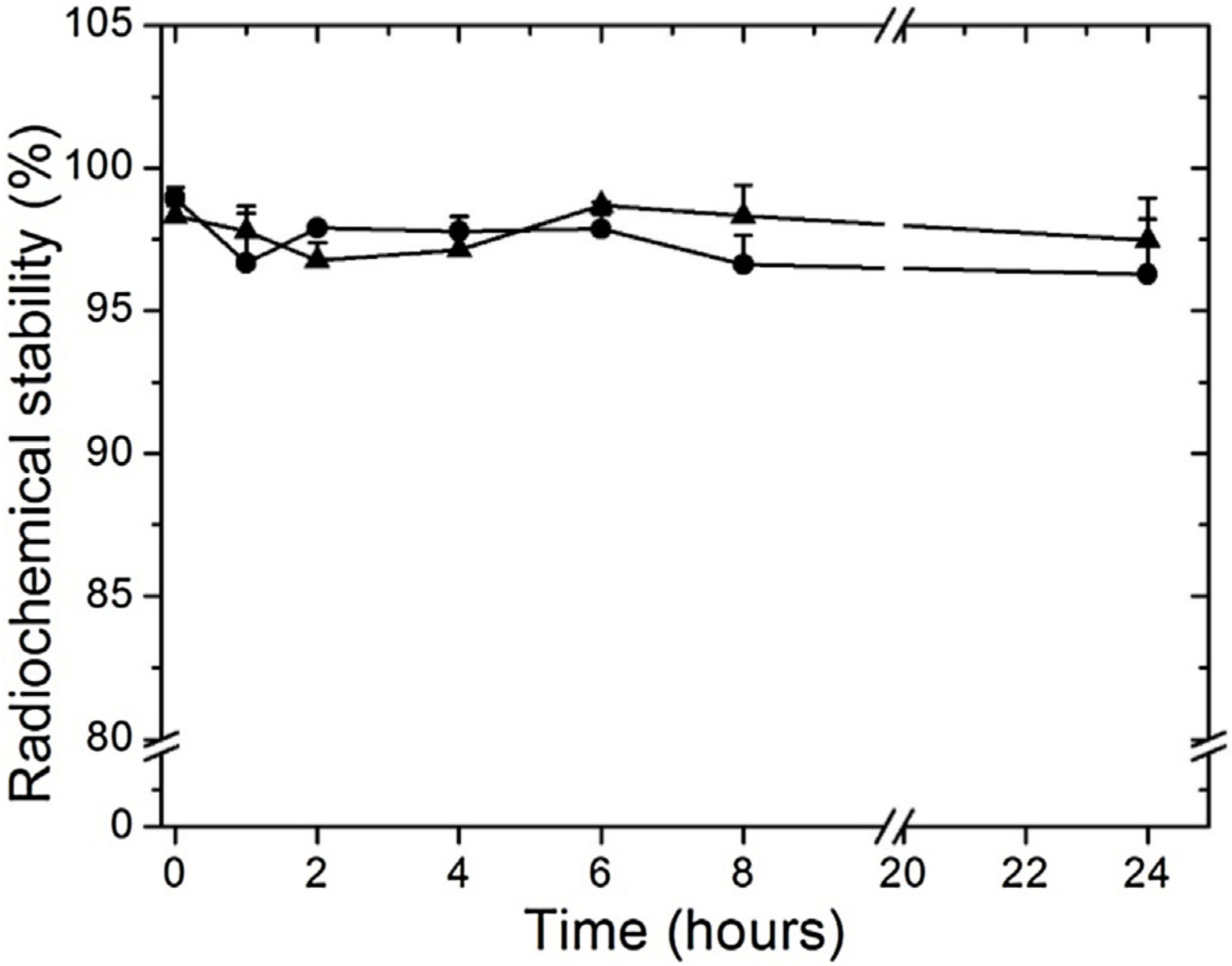

Fig. 1.

In vitro stability of ^{99m}Tc-PTX as a function of time in the presence of saline, at room temperature (triangle), or murine plasma, at 37 °C (circle) (n = 5).

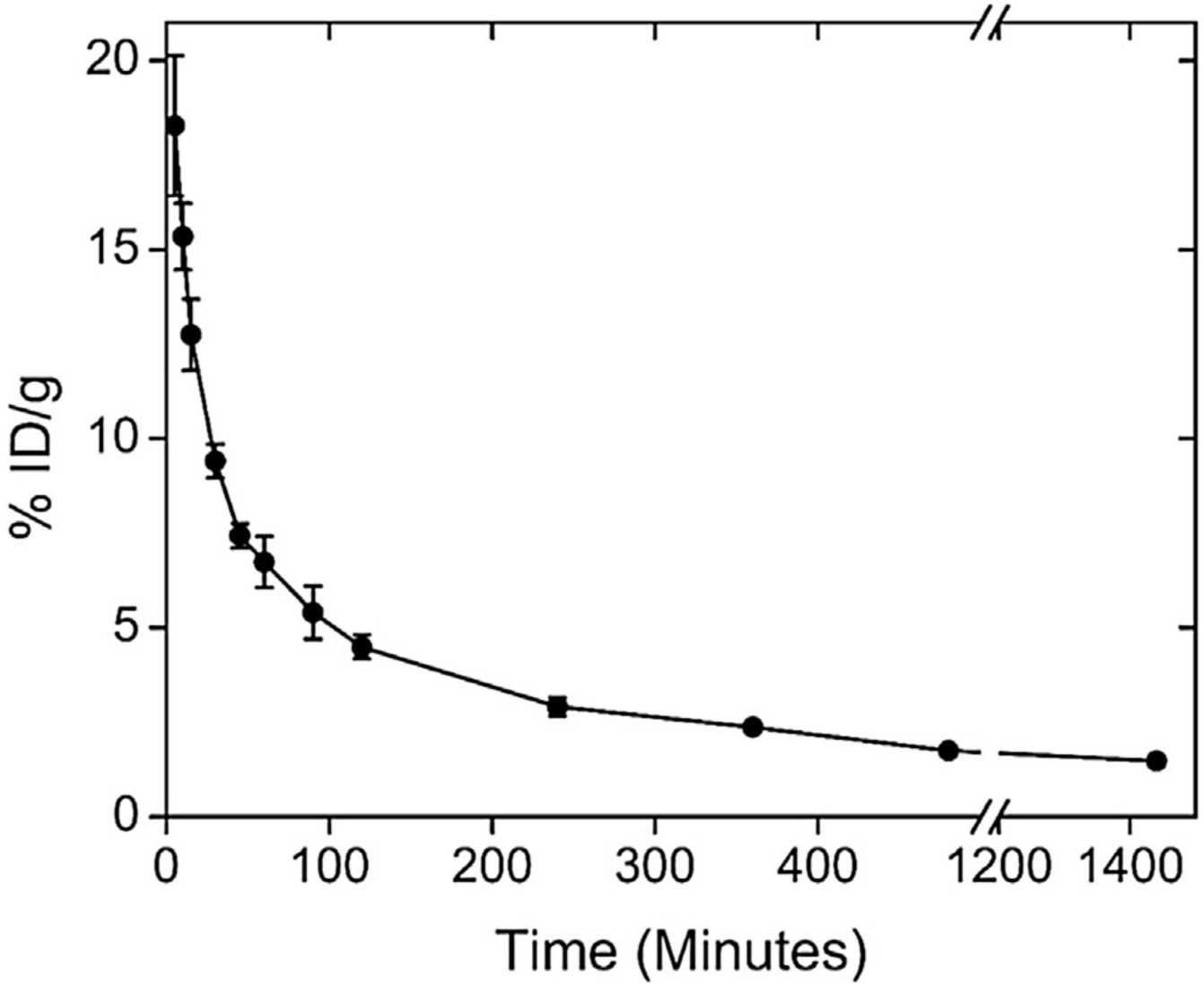

Fig. 2.

Blood clearance of ^{99m}Tc-PTX in healthy female BALB/c mice. All data points represent the mean percentage of injected dose of ^{99m}Tc-PTX ± SD (n = 7).

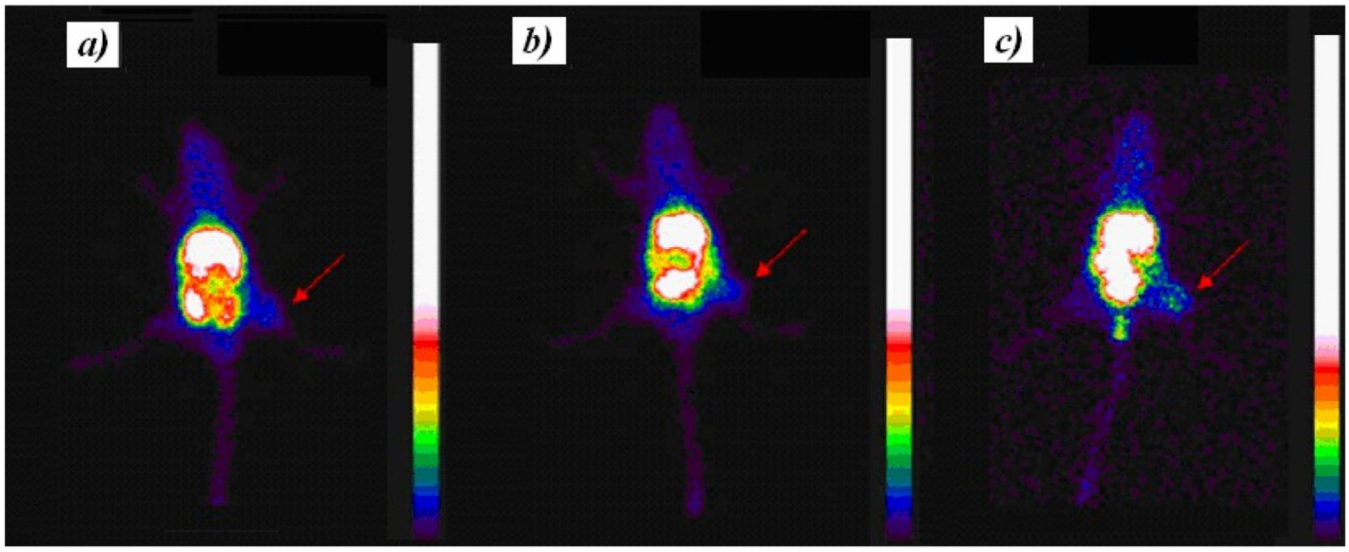

Fig. 3.

Scintigraphic images obtained at 4 (a), 8 (b), and 24 (c) h post-injection of ^{99m}Tc-PTX in tumor-bearing female BALB/c mice. Arrows indicate tumor area.

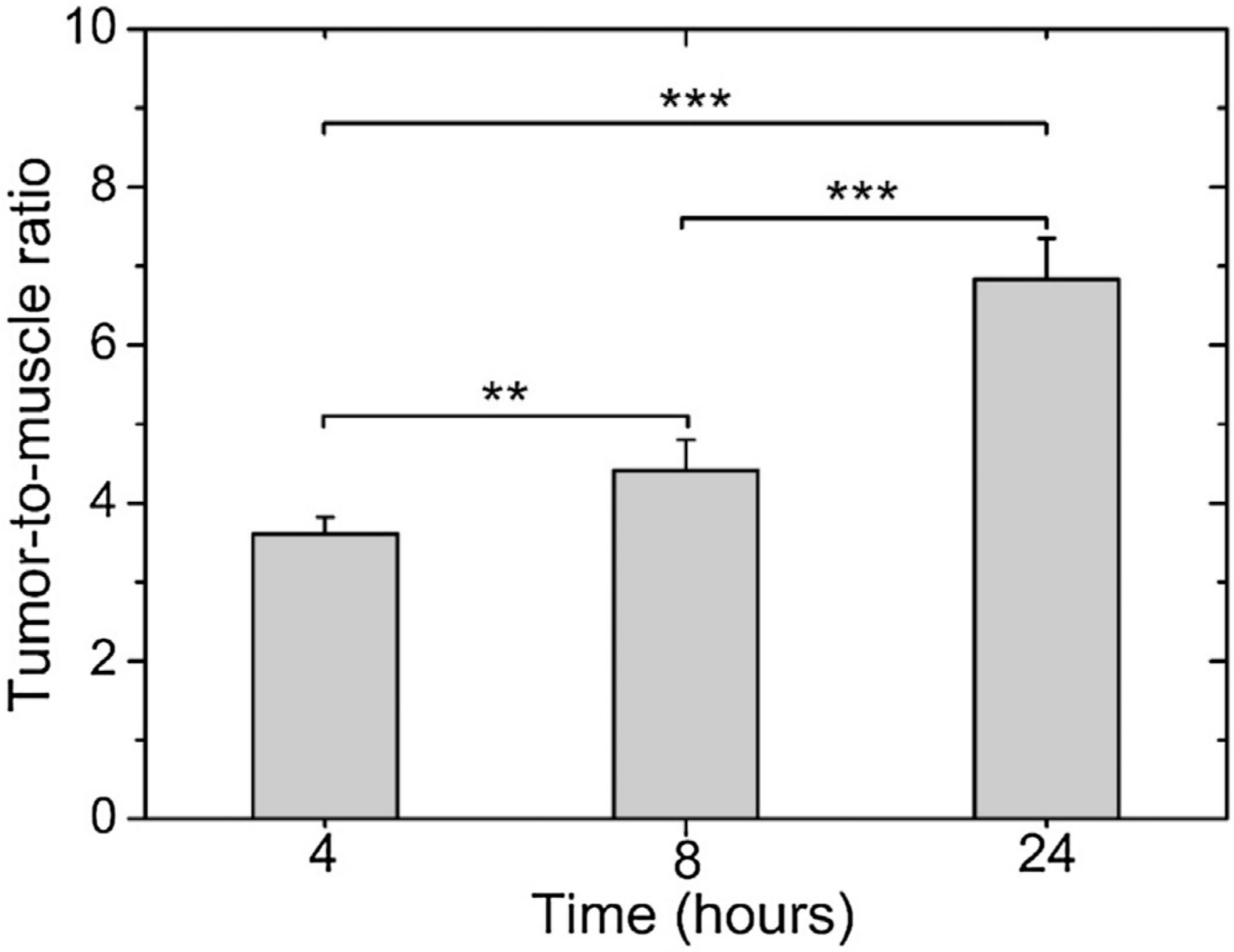

Fig. 4.

Tumor-to-muscle ratios determined by scintigraphic images at 4, 8, and 24 h post-injection of ^{99m}Tc-PTX in tumor-bearing mice. Asterisks indicate significant difference (**$p < 0.01$; ***$p < 0.001$).

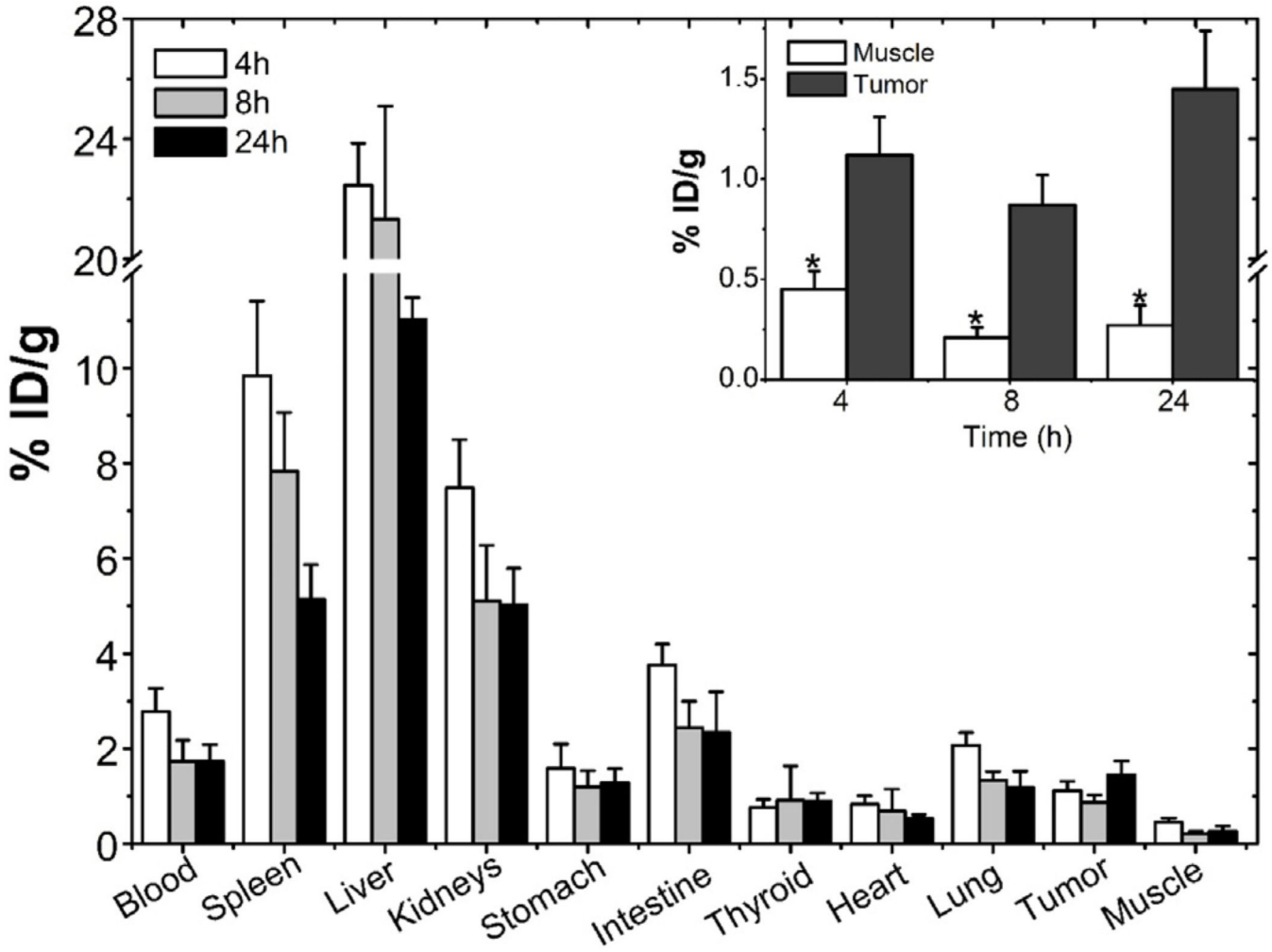

Fig. 5.

Biodistribution profile of ^{99m}Tc-PTX at 4, 8, and 24 h post-injection in tumor-bearing mice. Inset: Tumor and muscle uptake. Asterisks indicate significant difference between the tumor and muscle uptake at the same time point ($p < 0.001$). Bars represent mean percentage of the injected dose of ^{99m}Tc-PTX per gram of tissue ± SD ($n = 7$).